To study properties of supported clusters on a fundamental level, one wishes to have
- monodisperse clusters
- equally spaced
- on substrate interacting not too strong with clusters

This would allow to address the clusters coherently, to address single clusters one-by-one and to study cluster-cluster interaction (Fig 16)
Methods for fabrication of supported clusters are (Fig 5.16)

- deposition of mass selected clusters (i)
- deposition of clusters in an organic shell (ii)
- self organisation (iii)

The methods (i) and (iii) are visualized by Figs. 5.17 – 5.24

5.8. Clusters in Catalysis

Due to the large surface to volume ratio clusters are expected to be catalytically active in heterogeneous catalysis, if the number of produced product molecules is normalized with the number of catalyst atoms.
In addition electronic structure and crystal structure are a strong function of cluster size, and thus one might expect this changing structures to cause a pronounced size dependence of reactivity
Let us consider a few examples

- Mass-selected Pt clusters on MgO show a clear maximum in the catalytic activity for CO oxidation for a cluster size of about 15 atoms. The increase in catalytic activity with cluster size is associated with a transition from two dimensional to three dimensional clusters. The key process in CO oxidation is the O_2 dissociation This process can be expected to become most effective if the partially populated antibonding π_g^* orbital of O_2 forms a resonance

with the cluster density of states. As shown by density functional theory the large and narrow d-band position is most relevant. As shown in Fig. 25, the center of the Pt d-band coincides roughly with the π_g^* O_2 orbital for a cluster size of about 15.
It is noteworthy that the CO_2 molecule production per Pt atom of 0.4 for 15 atom Pt clusters is twice as high as for a flat (111) surface.

- While bulk Au is unable to catalyze any chemical reaction, Au clusters catalyze a number of reactions. Au-clusters are the most efficient catalyst for CO oxidation at low temperatures. Fig. 26 displays Au-clusters created by evaporation and annealing to 850K on TiO_2 (110) – (1×1). Scanning tunneling spectroscopy shows that Au-clusters with diameters below about 3 nm display a bandgap. A detailed analysis shows that monolayer thick Au-clusters exhibit very large bandgaps, three layer clusters are metallic while two layer clusters have bandgaps of 0.2–0.6 eV and are of the size range where catalytic activity is highest. It is inferred that the opening of the band-gap gives rise to the catalytic activity.

- Reasonably regular arrangements of Au-clusters were achieved by adsorption of micelles containing Au-clusters on SiO_2. Subsequent application of an O-plasma removed the organic shell and left the metal Au. While the XPS of 4f-levels shows Au_2O_3 formation for the flat Au (111) and most cluster sizes, for the Au_{55} cluster (which can be prepared precisely) no oxide is formed. The Au_{55} clusters are still metallic and thus this effect may be attributed to a magic cluster size, the closed shell ikosaeder of Au_{55}.

5.9 Clusters for Data Storage

While current hard disk drives store each magnetic bit to an ensemble of randomly positioned grains of a magnetic thin film, as storage density

will increase to the ultimate, one may envision that each bit is stored on a single accurately positioned magnetic cluster (Fig. 5.28). For a usable magnetic storage device a storage time τ of about 10 years $= 3 \cdot 10^8$ s is required. Using our simplistic model for the fluctuation of the magnetic orientation we have

$$\tau = \tau_0 \, e^{K_{an}V/kT}$$

where K_{an} is the magnetic anisotropy energy density $E_{an} = K_{an} \cdot V$. With $\tau_0 \approx 10^{-10}$ s we arrive at $\frac{K_{an} \cdot V}{kT} \approx 42$. With $kT \approx k \cdot 350K \approx 0{,}03$ eV we arrive at $K_{an} \cdot V \approx 1{,}2$ eV. For a minimal volume of our magnetic bit we thus need a material with a maximum K_{an}. Probably the most promising material is FePt in the L_{10}-phase. It is a face centered tetragonal phase with alternating Fe and Pt (100) layers and $K_{an} = 7 \cdot 10^6$ J/m³ $= 1{,}1 \cdot 10^{26}$ eV/m³.
With $V = l^3 = \frac{1{,}2 \text{ eV}}{K_{an}}$ we arrive at $l \approx 2{,}5$ nm. This value presents the ultimate size of a magnetic bit if the clusters do not interact, which has to be ensured by a suitable spacer layer. Experimentally for 4 nm particles a ratio $\frac{K_{an} \cdot V}{k \cdot 300K} = 48$ has been realized yielding $K_{an} = 5{,}9 \cdot 10^6$ J/m³. As Fig. 5.29 displays, using clever chemical synthesis routes, FePt micelle particles may be arranged in a rather regular lattice. By heating the thermodynamically stable FePt $L1_0$-Phase is formed, which displays the desirable properties (e.g. large coercitive fields). The annealing temperatures of about 600°C required to establish the $L1_0$-phase are still prohibitive for practical applications. Besides this and other material problems still the problem of reading and writing to such bits is unsolved. Fig. 5.30 shows measurements for magnetization and hysteresis as a function of temperature and particle size, visualising the ferromag. → superparamag. transition

6. Thin Films ; 6.1 Polycrystalline vs Epitaxial Films

Thin films is a discipline in its own in the range of applied physics. We will treat thin films here from a surface science point of view with an emphasis on atomic scale processes. Thin film growth and fabrication is a field of an enormous range of applications:

- hard coatings (for tools)
- low-E thin films (for windows)
- anti-reflection coatings (lenses)
- x-ray mirrors (science, EUV optics)
- microelectronic devices (computer industry)
- thin film solar cells (regenerative energy)
- optoelectronic devices (laser diodes, OLED's)
- 2D electron gas heterostructures (research, instruments)

See Figs. 6.1+6.2 - oxide thin films (Tunneling contacts, MRAM)
- magnetic films (Data Storage)

We consider now different scenarios of thin film growth

(i) polycrystalline thin films on an amorphous substrate

This is a typical situation for low-tech applications. Important steps in film formation are

- nucleation
- growth
- coalescence
- grain growth
- abnormal grain growth

All these processes reduce energy under the constraint of limited atomic mobility. See Fig. 6.3

Although the amorphous substrate by itself does not induce orientation of the crystallites, it is often observed that the grains orient themselves. We talk of out of plane texture, if

if the grains are oriented with respect to the substrate plane and of in-plane texture, if they are oriented within the substrate plane. Such biaxially oriented grains form a „quasi" single crystal film. Their properties are often superior to films with randomly oriented grains (e.g. in the case of low-E films biaxial texture is desirable).

side view

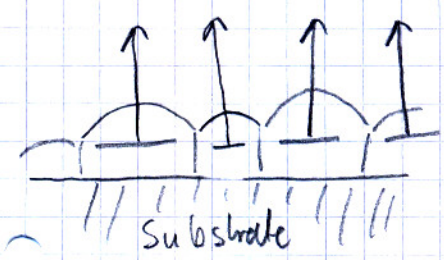

out-of-plane texture

top view

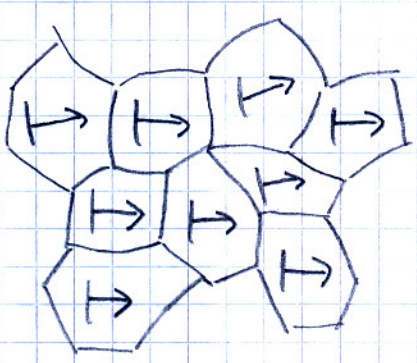

in-plane texture

Certainly the structure of a thin film depends on the growth temperature. A good way to characterize the growth temperature is to scale the growth temperature with the melting temperature T_m: $T_{scaled} = \frac{T}{T_M}$ Fig. 6.4 displays our current understanding of the grain structure in thin films. Secondary nucleation, i.e. the nucleation of differently oriented grains on existing ones at elevated temperatures takes only place by heterogenous nucleation at impurities. This is visualized in the lecture through a TEM growth movie.

(ii) epitaxial thin film growth.

„epi" „taxis" is greek and means order („taxis") takes place upon („epi") something. Epitaxy is ordered overgrowth and we distinguish heteroepitaxy =: substrate ≠ deposit

homoepitaxy =: substrate = deposit

Epitaxy is characterized by the following relations:

- planes of substrat and deposit are parallel
- directions of substrate and deposit are parallel
- there exists an approximate coincidence mesh for substrate and deposit
- in epitaxial thin films often elastic deformations are of great importance. For a pseudomorphic (1:1 relation of substrate and deposit lattices) film a deviation of the natural deposit lattice parameter a_d from the substrate lattice parameter a_s is accomodated by straining the deposit. The misfit

$$m = \frac{a_s - a_d}{a_d} = \varepsilon$$

is the deposit strain. In general, the misfit is the deviation of the deposit from the coincidence lattice defined by the substrate mesh a_s. Note that misfits generally depend on orientation and it must be specified for two directions. Figs 6.5+6.6 display the well known example for the epitaxy of rutile (TiO_2) on hematite (Fe_2O_3). In case of only weak substrate-deposit interaction only very small misfits can be accomodated, resulting in large coincidence lattices.

Epitaxial films are of great importance for high-tec applications of thin films. Due to their structural perfection electron scattering and electron-hole pair recombination are reduced, resulting in superior electrical and optical properties.

A well known example for a technical system are Si - SiGe hetero-structures for high mobility transistors. The strained layers grow pseudomorphic on each other and allow to separate doping and electron transport